



WEAK NEUTRAL CURRENTS IN e^+e^- EXPERIMENTS

by

Albrecht Böhm

Erratum

A factor $\frac{3}{8}$ has been omitted in formulae (13), (16), and (17).
The correct expressions are

page 16

$$A_{\mu\mu} = \frac{3}{2} \times g_A^e g_A^\mu \quad (13)$$

page 28

$$A_{\tau\tau} = \frac{3}{8} \frac{B}{R_{\tau\tau}} \quad (16)$$

and

$$A_{\tau\tau} = \frac{3}{2} \times g_A^e g_A^\tau \quad (17)$$

DEUTSCHES ELEKTRONEN-SYNCHROTRON DESY

DESY 82-084
December 1982



WEAK NEUTRAL CURRENTS IN e^+e^- EXPERIMENTS

by

Albrecht Böhm

Deutsches Elektronen-Synchrotron DESY, Hamburg

and

III. Physikalisches Institut, RWTH Aachen

ISSN 0418-9833

NOTKESTRASSE 85 · 2 HAMBURG 52

**DESY behält sich alle Rechte für den Fall der Schutzrechtserteilung und für die wirtschaftliche
Verwertung der in diesem Bericht enthaltenen Informationen vor.**

**DESY reserves all rights for commercial use of information included in this report, especially in
case of filing application for or grant of patents.**

To be sure that your preprints are promptly included in the
HIGH ENERGY PHYSICS INDEX,
send them to the following address (if possible by air mail) :

**DESY
Bibliothek
Notkestrasse 85
2 Hamburg 52
Germany**

WEAK NEUTRAL CURRENTS IN e^+e^- EXPERIMENTS

Albrecht Böhm

Deutsches Elektronen Synchrotron DESY
D2000 Hamburg 52 Fed. Rep. Germany

and

III. Physikalisches Institut, RWTH Aachen
D5100 Aachen, Fed. Rep. Germany

(Presented at the SLAC Summer Institute on Particle Physics,
Stanford, California, August 1982)

ABSTRACT

Results on weak neutral currents in e^+e^- reactions at PETRA and PEP are reviewed. A study of the leptonic reactions $e^+e^- \rightarrow \ell^+\ell^-$ leads to the conclusion that the electron, muon and tau lepton interact as if pointlike with cross sections, which are in agreement with the standard electro-weak theory of Glashow, Salam and Weinberg. A very significant forward-backward asymmetry of the reaction $e^+e^- \rightarrow \nu^+\mu^-$ measured by three PETRA experiments JADE, MARK-J and TASSO. Their combined value is $A_{\mu\mu} = (-10.4 \pm 1.4)\%$ in good agreement with the standard model which predicts -9.3% . PETRA experiments including CELLO also measure a significant asymmetry, $A_{\tau\tau} = (-7.9 \pm 2.2)\%$, in the reaction $e^+e^- \rightarrow \tau^+\tau^-$ in accord with the GSW model and e,ν,τ universality. A fit to the cross sections of $e^+e^- \rightarrow ee$ and $e^+e^- \rightarrow \mu\mu$ at $s = 1200 \text{ GeV}^2$ gives $\sin^2 \theta_W = 0.27 \pm 0.07$ and tests the standard model at very high energies. Finally, first attempts have been made to extend these studies to hadronic reactions $e^+e^- \rightarrow q\bar{q}$ with the aim of measuring the weak neutral current couplings of heavy quarks.

I. INTRODUCTION

Weak neutral currents have been extensively studied in neutrino reactions (1,2) and electron-deuteron scattering (3). The results give strong support to the standard $SU(2)_L \times U(1)$ theory (WS-GIM model) (4). One therefore may ask what we learn by measurements of e^+e^- reactions at PETRA and PEP, where the c.m.

energy \sqrt{s} is below the Z^0 mass. A simple answer is that it is always necessary to check a theory over the whole range of interactions where it makes predictions. A quantitative answer is that one tests the theory at q^2 and s which are much higher in the $e^+ e^-$ reaction than in other fields. In addition, the reactions $e^+ e^- \rightarrow l^+ l^- (\ell = e, \mu, \tau)$ are purely leptonic reactions and are free from the complications due to strong interactions appearing in neutrino-nucleon scattering. They should therefore be compared to neutrino-electron scattering and, as we will see later, the data have now reached the precision of the ν - e measurements (5). It should also be added that the measurements of $e^+ e^- \rightarrow l^+ l^-$ test the $e-\mu-\tau$ universality. Similar arguments can be made for the reaction $e^+ e^- \rightarrow q\bar{q} \rightarrow$ hadrons, where we hope to measure the weak coupling constants of the heavy quarks c, b and the as yet undiscovered top quark. Last but not least the PETRA and PEP storage rings operate at energies where for the first time we might be able to observe a deviation from the point-like four-fermion coupling.

Clearly, such a deviation would either show the compositeness of leptons or, as expected, indicate the existence of the Z^0 boson. This would be an important step in our understanding of weak interactions.

There is one difficulty when we try to study weak neutral currents with charged leptons: the cross sections are dominated by the electromagnetic interaction due to their charges and the purely weak interaction is negligibly small. However, the cross section also contains an interference term between the γ and Z^0 exchange, which rises linearly with s relative to the pure QED cross section and

becomes measurable at c.m. energies of 30 to 40 GeV.

Finally it should be noted that there have been extensive searches for new particles in high energy $e^+ e^-$ reactions (6). Many results are relevant to the theory of weak interaction. Although these searches cannot be discussed thoroughly in this talk owing to the limited time, the most relevant results should be mentioned. No leptons more massive than the tau, nor quarks heavier than the bottom have been found up to c.m. energies of 36 GeV. It would also be very exciting to find scalar or pseudoscalar particles which test our ideas about gauge symmetry breaking. Neutral Higgs particles can only be detected at the toponium and at the Z^0 peak or above. However, extensive searches for charged Higgs particles and technipions have been performed at PETRA, PEP and CESR. The result is that their existence is excluded for masses between the tau mass and 13.5 GeV independently of their decay branching ratios into $\tau\nu$, $c\bar{s}$ or $c\bar{b}$.

In the following chapters we will discuss the results of the individual leptonic reactions. The central point will be the measurements of the forward-backward asymmetry in the reaction $ee \rightarrow \nu\nu$ and $ee \rightarrow \tau\tau$. We will also combine all data on leptonic $e^+ e^- \rightarrow \nu\nu$ and compare them with neutrino-electron scattering. In the last chapter we will report on first attempts to extend these measurements to the hadronic reaction $ee \rightarrow qq$ with the aim of determining the neutral current couplings of heavy quarks.

II. NEUTRAL CURRENT COUPLINGS OF LEPTONS

The reaction $e^+ e^- \rightarrow l^+ l^-$ is described in a model-independent way by three parameters. Following Hung and Sakurai (7) we call them h_{VV} , h_{VA} and h_{AA} . Clearly, if we use the same parameters for electron, muon and tau lepton, we assume lepton universality of the weak neutral currents. At high energies we have to introduce the Z^0 masses as additional parameters. If we only discuss models with a single Z^0 , we can relate the parameters h_{VV} , h_{VA} and h_{AA} to the vector and axial vector couplings g_V , g_A , measured in neutrino-electron scattering (factorization). If the coupling constant of the neutrino to the Z^0 is given by $c_\nu/2$, we then have the following relations

$$\begin{aligned} h_{VV} &= \frac{g_V^2/c_\nu^2}{g_A^2/c_\nu^2} & h_{VA}^2 = h_{VV} \cdot h_{AA} &= \frac{g_V^2 g_A^2/c_\nu^4}{\rho} \\ h_{AA} &= \frac{g_A^2/c_\nu^2}{g_V^2/c_\nu^2} & \rho &= 1.002 \pm 0.015 \quad \text{and} \quad \sin^2 \theta_W = 0.234 \pm 0.013 \end{aligned} \quad (1)$$

Thus in theories with a single Z^0 , the reactions $e^+ e^- \rightarrow l^+ l^-$ are described by three parameters, the two coupling constants h_{VV} , h_{AA} and the mass of the Z^0 boson.

In $SU(2) \times U(1)$ models these parameters are expressible in terms of the weak mixing angle $\sin^2 \theta_W$ and of the weak isospin components of left handed and right handed leptons.

$$h_{VV} = \rho (T_{3L} + T_{3R} + 2 \sin^2 \theta_W)^2 \quad (2)$$

$$\begin{aligned} h_{AA} &= \rho (T_{3L} - T_{3R})^2 \\ m_Z^2 &= \frac{1}{\rho} \frac{\pi \alpha}{\sqrt{2} G_F} \frac{1}{\sin^2 \theta_W \cos^2 \theta_W} \end{aligned} \quad (2)$$

The parameter ρ measures the strength of the weak neutral current interaction relative to the weak charged current interaction. We can also rewrite the third relation of (2) as

$$\rho = \frac{m_W^2}{m_Z^2 \cos^2 \theta_W} \quad (3)$$

where m_W is the mass of the charged vector boson. A combined fit to neutrino electron and electron deuteron measurements leads to (2)

$$\rho = 1.002 \pm 0.015 \quad \text{and} \quad \sin^2 \theta_W = 0.234 \pm 0.013 \quad (1)$$

Assuming $\rho = 1$ expressions (2) become

$$h_{VV} = (T_{3L} + T_{3R} + 2 \sin^2 \theta_W)^2 \quad (4)$$

$$h_{AA} = (T_{3L} - T_{3R})^2 \quad (4)$$

In the standard $SU(2)_L \times U(1)$ theory of GSW (4) the left-handed lepton fields are arranged in weak iso-doublets, the right-handed lepton fields in weak iso-singlets. Since this theory also predicts $\rho = 1$, we get

$$\begin{aligned} h_{VV} &= g_V^2 = \frac{1}{4} (1 - 4 \sin^2 \theta_W)^2 \\ h_{AA} &= g_A^2 = \frac{1}{4} \end{aligned} \quad (5)$$

Using $\sin^2 \theta_W = 0.23$, we find that $g_V^2 = 0.002$, $g_A^2 = 0.25$ and $m_Z^2 \sim 90$ GeV.

The leptonic cross sections in $e^+ e^-$ reactions depend on the square of the vector or axial-vector coupling constant, but we cannot detect an effect due to the vector coupling, because it vanishes. However, the reverse argument is also valid: if we see no effect due to g_V^2 , the weak mixing angle $\sin^2 \theta_W$ has to be very near to 0.25, in order to give $g_V^2 \sim 0$. The parameters h_{VV} and h_{AA} are often called g_V^2 and g_A^2 in $e^+ e^-$ experiments and we follow that usage. However, be warned that the symbols g_V and g_A are usually reserved for the coupling constants of ν - e scattering. It should be noted that the vector and axial vector couplings in $e^+ e^-$ experiments are determined independently of assumptions about c_V the coupling of the Z^0 to neutrinos. The parameter c_V and expression (1) should be employed if the vector and axial-vector coupling constants measured in $e^+ e^-$ experiments are compared with those measured in neutrino-electron experiments.

As an example of the dependence of a cross section on these parameters, we will discuss the cross section for the reaction $ee \rightarrow \mu\mu$ or $ee \rightarrow \tau\tau$. If we define θ as the polar angle of the μ^- with respect to the outgoing e^- beam, then the μ^- angular distribution has the following form:

$$\frac{d\sigma}{d\cos\theta} = \frac{\pi\alpha^2}{2s} \left[R_{\mu\mu} (1+\cos^2\theta) + B\cos\theta \right] \quad (6)$$

$$\text{where } R_{\mu\mu} = \sigma_{\mu\mu} / \frac{4\pi\alpha^2}{3s} = 1 + 2g_V^2 \chi + (g_V^2 + g_A^2) \chi^2$$

$$\text{and } \chi = \frac{G_F}{2\sqrt{2}\pi} \frac{s \cdot m_Z^2}{s - m_Z^2} \approx -0.26 \text{ for } \sqrt{s} = 35 \text{ GeV}, m_Z = 90 \text{ GeV.}$$

The factor

$$B = 4 \frac{g_A^2 \chi}{g_V^2} + 8g_V^2 g_A^2 \chi^2 \quad (8)$$

depends mainly on the axial vector coupling and it determines the forward-backward asymmetry which is given by

$$A_{\mu\mu} = \frac{N(\theta < 90^\circ) - N(\theta > 90^\circ)}{N(\theta < 90^\circ) + N(\theta > 90^\circ)} = \frac{3}{8} \frac{B}{R_{\mu\mu}} \quad (9)$$

$N(\theta < 90^\circ)$ is the number of events, where the μ^- is in the forward hemisphere, defined by the outgoing e^- beam.

This asymmetry depends on g_A^2 and is practically independent of the value of g_V^2

$$A_{\mu\mu} = \frac{3}{8} \frac{B}{R_{\mu\mu}} = \frac{3}{8} \frac{4g_A^2 \chi (1+2g_V^2 \chi)}{(1+2g_V^2 \chi + \dots)} \approx \frac{3}{2} \frac{g_A^2 \chi}{\chi} \quad (10)$$

Lepton universality is assumed in expressions (6) to (10), otherwise one should replace g_A^2 by $g_A^2 g_\ell^2$ and g_V^2 by $g_V^2 g_\ell^2$, where ℓ is the lepton produced in the final state. The asymmetry is negative and its absolute value increases with s . At $\sqrt{s} = 35$ GeV we calculate a value of $A_{\mu\mu} = -9.7\%$ for $g_A^2 = 1/4$ and $m_Z = 90$ GeV. The asymmetry depends weakly on the Z^0 mass owing to the propagator term included in the variable χ . If we set the Z^0 mass to infinity, we expect an asymmetry of -8.2% . Clearly asymmetries of this size are measurable, but it will be very hard to prove that the Z^0 mass is finite with a value around 90 GeV. However, this question may be answered in the near future by the new measurements at PETRA at the end of 1982 when the energy is to be raised to $\sqrt{s} = 40$ GeV. The corresponding values for the asymmetry

- 7 -

at $\sqrt{s} = 40$ GeV are -13.5% or -10.8%, for a Z^0 mass of 90 GeV or infinitely large, respectively.

III. MEASUREMENT OF LEPTONIC REACTIONS

We will now discuss the measurements of the leptonic reactions.

Table I lists the basic experimental conditions for the experiments at PEP and PETRA.

STORAGE RING	EXPERIMENTS	ENERGY	Ldt
PEP	MAC, MARK II	$\sqrt{s} = 29$ GeV	20-30 pb ⁻¹
PETRA	CELLO, JADE, MARK-J, PLUTO, TASSO	$\langle \sqrt{s} \rangle = 34.5$ GeV	50-70 pb ⁻¹

TABLE I Experiments and Their Basic Running Conditions at PEP and PETRA

The experiments at DESY have had the advantage that the PETRA storage ring has operated at a higher energy and has delivered a higher integrated luminosity.

In the framework of this talk it is not possible to describe the experiments and the details of the event selection. The reader is referred to publications of the individual experiments (8-14). Leptonic events are easily recognized as two collinear back-to-back leptons, whose momenta are approximately equal to the beam momentum.

For selection one typically requires the acollinearity angle ξ to be smaller than 10° and the lepton momentum to be larger than half the beam momentum. The radiative corrections to order α^3 are calculated for these cuts by the Monte Carlo program of Berends and Kleiss (15).

IV. RESULTS ON $e^+e^- \rightarrow e^+e^-$

We begin our discussion of individual leptonic reactions with Bhabha scattering, $e^+e^- \rightarrow e^+e^-$. Its measurement fulfills a twofold purpose: small angle Bhabha scattering serves as a luminosity monitor, while the angular distribution at large angles is sensitive to the weak interaction. The theoretical cross section (16) shows a rather complicated dependence on g_V^2 and g_A^2 because there are space-like and time-like exchanges of the virtual photon and the Z^0 . As an example of the sensitivity of Bhabha scattering to the weak interaction Fig. 1 indicates the deviation from QED for two values of the vector coupling, $g_V^2 = 0$ or $g_V^2 = 1/4$, while the other parameters are $g_A^2 = 1/4$ and $m_Z = 90$ GeV. The shape of the angular distribution of Bhabha scattering depends mainly on the vector coupling. This behaviour is opposite to that of the angular distribution of the reaction $ee \rightarrow \mu\bar{\mu}$ in which the axial vector coupling g_A is dominant. We note that the weak interaction modifies Bhabha scattering only a few percent. Therefore, we do not present the results from Bhabha scattering alone, but determine the vector and axial vector couplings from a combined fit of all leptonic reactions. Since this is done in chapter IX, we only show here examples of the existing data. Fig. 2 displays the angular

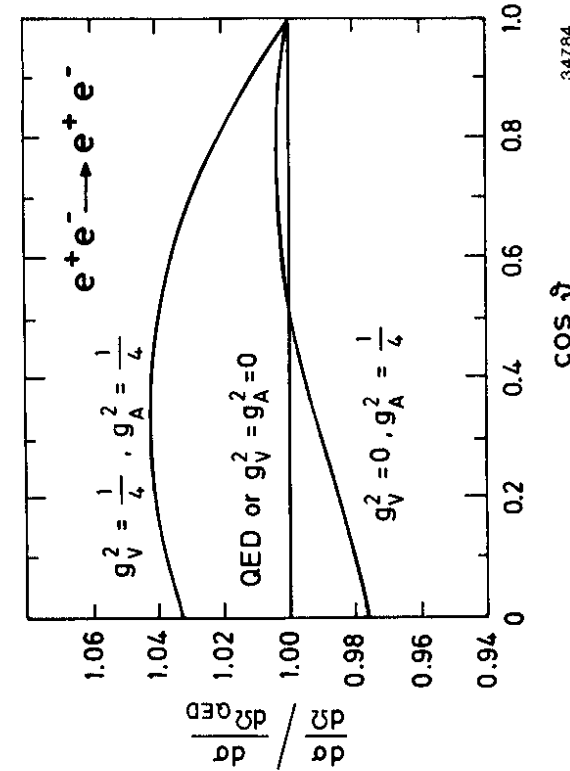


Fig. 1 Examples of how the weak interaction effects the differential cross section for Bhabha scattering, which is normalized by the QED cross section $\frac{d\sigma_{QED}}{d\Omega}$. The predictions for different values of the vector and axial vector couplings are shown. The Z^0 mass is 90 GeV. The angular distribution is folded around $\theta = 90^\circ$, as would be the case for experiments which do not measure the charge of the electron.

distribution of Bhabha scattering measured by the MAC experiment (13) at PEP. The results of the PETRA experiments are shown in Fig. 3, where the ratio of the measured cross section to the calculated QED cross section is plotted. In this way deviations from QED are more visible. The errors indicated in Fig. 3 are only statistical. In addition, there are systematic errors on the overall normalization of 3 to 5% and point-to-point errors of 1 to 3% for the different experiments. Because the vector coupling g_V is expected to be negligibly small and the axial vector coupling modifies the cross section by less than 3%, we can not prove the existence of weak interaction in Bhabha scattering. However, we can use the measurements in a combined fit of all leptonic data to determine a limit on the vector coupling constant.

V. CROSS SECTION OF $e^+e^- \rightarrow \mu\mu$

The results on the reaction $e^+e^- \rightarrow \mu\mu$ can be divided into two parts, the total cross section $\sigma_{\mu\mu}$ and the forward-backward asymmetry $A_{\mu\mu}$. We first consider the cross section, where we present the results in terms of $R_{\mu\mu}$, the cross section normalized to the point-like cross section. The systematic error on $R_{\mu\mu}$ is dominated by an overall normalization error due to luminosity and acceptance, which ranges between 3% and 5% for different experiments. The statistical error at the highest energies of $\sqrt{s} \approx 34.5$ GeV is about 2% as typically 3000 muon pairs are observed.

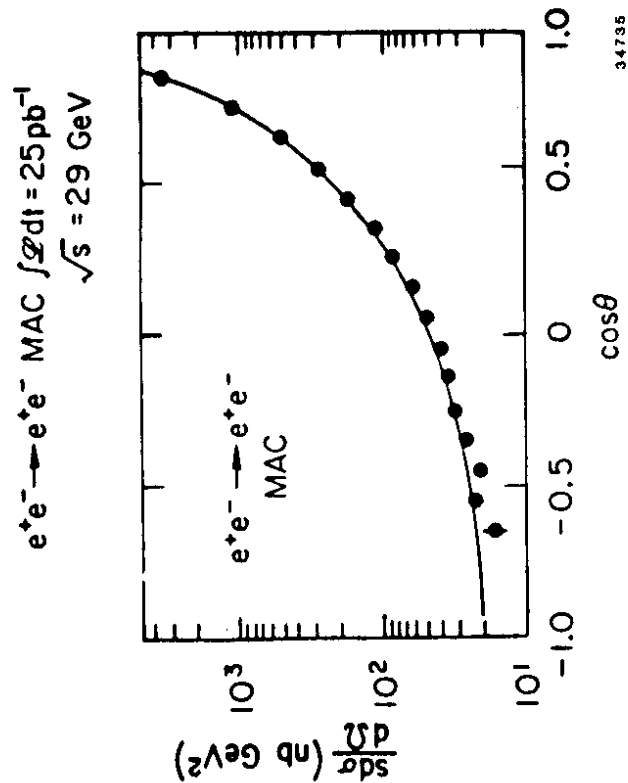


Fig. 2 Differential cross section of Bhabha scattering measured by the MAC group (13) at PEP.

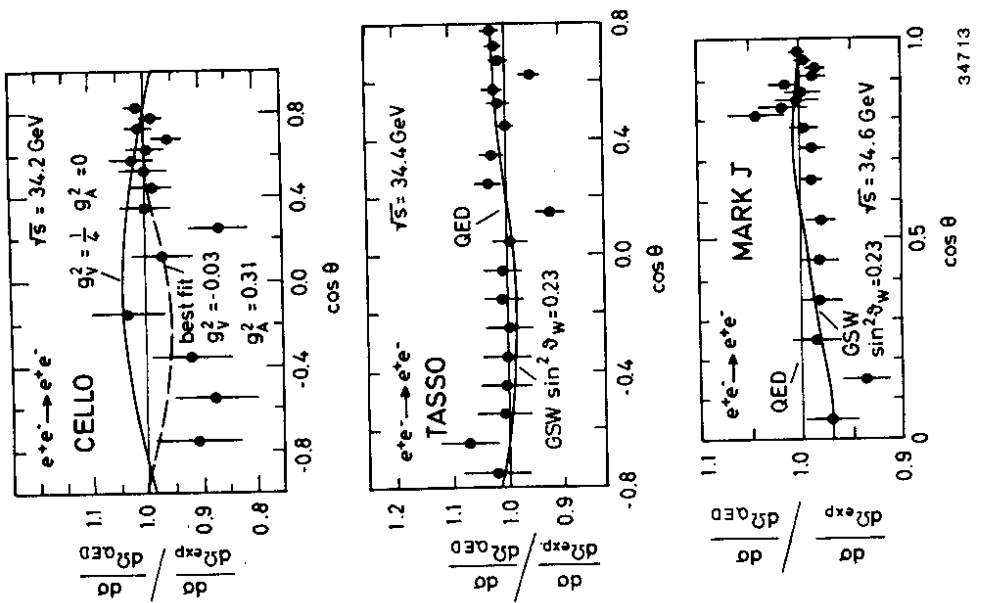


Fig. 3 Measurements of Bhabha scattering by the PETRA experiments CELLO, TASSO and MARK-J. The measured cross section is divided by the theoretical QED cross section and compared to the predictions of the electroweak theory.

34713

The effect of the weak interaction on the cross section depends mainly on the vector coupling of the electron and the muon. From (7) we read off the approximation for the deviation $\Delta R_{\mu\mu}$ from the QED cross section $R_{\mu\mu} = 1$.

$$\Delta R_{\mu\mu} \approx 2 \lambda g_V^{\mu} \quad (11)$$

Therefore no deviation from QED can be observed, if the vector coupling of the muon or the electron vanishes. This would be the case for $\sin^2 \theta_W = 0.25$. In the other extreme case of $g_V^2 = 1/4$ we should observe a decrease of the cross section by 13%. The cross sections measured at PETRA at the three energies, $\sqrt{s} = 14, 22$ and 34.5 GeV are shown in Fig. 4. The measurements agree with the pure QED prediction within the statistical and systematical errors. This result can be interpreted in two ways: first, if we assume the validity of QED, we find that the vector coupling g_V is very small and $\sin^2 \theta_W$ is near 0.25.

Detailed numbers will be given later for the combined fit to all leptonic reactions; second, if we neglect the weak interaction, which would in any case be unmeasurable for $\sin^2 \theta_W = 0.23$, we can test QED.

This is usually done in terms of a form factor writing

$$\sigma_{\mu\mu} = \sigma_{\text{QED}} \cdot F(s), \text{ where } F(s) = 1 + \frac{s}{s-\Lambda} \quad (12)$$

The agreement of the cross section with the QED prediction can then be expressed by a lower limit (95% C.L.) of the cut-off parameter Λ , which ranges between 150 and 200 GeV for different experiments. This value indicates, using the Heisenberg Uncertainty principle, that muons (and electrons) behave as point-like particles down to a distance 10^{-16} cm.

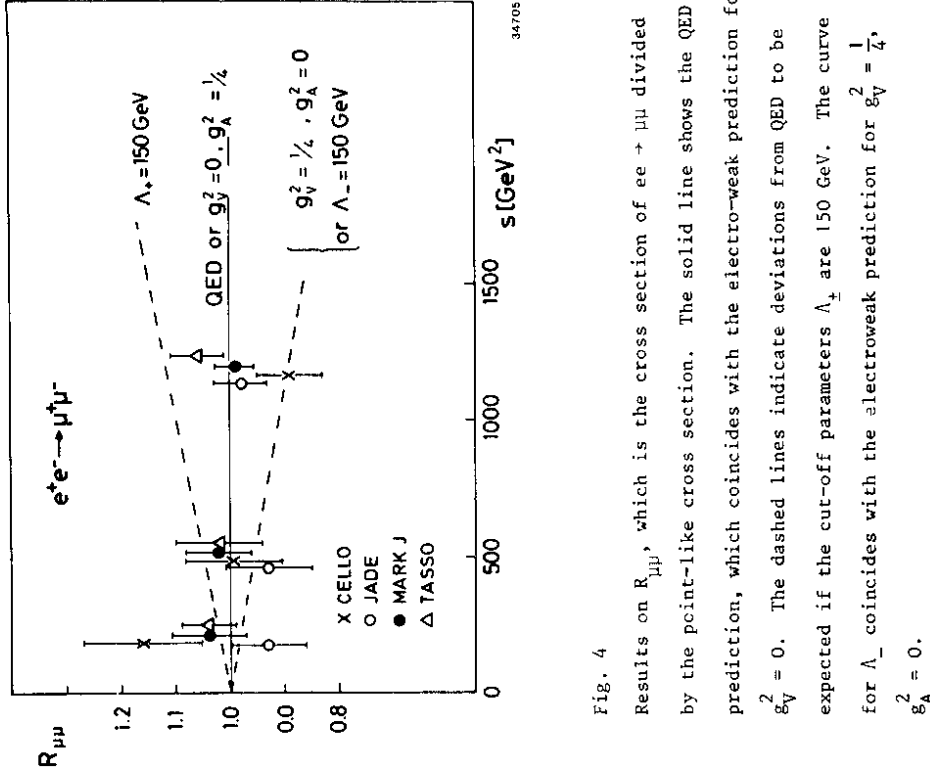


Fig. 4

Results on $R_{\mu\mu}$, which is the cross section of $e^+e^- \rightarrow \mu^+\mu^-$ divided by the point-like cross section. The solid line shows the QED prediction, which coincides with the electro-weak prediction for $g_V^2 = 0$. The dashed lines indicate deviations from QED to be expected if the cut-off parameters Λ_{\pm} are 150 GeV. The curve for Λ_- coincides with the electroweak prediction for $g_V^2 = \frac{1}{4}$, $g_A^2 = 0$.

VI. ASYMMETRY OF $e^+e^- \rightarrow \mu^+\mu^-$

The measurement of the forward-backward asymmetry is one of the central experimental tasks at high energy e^+e^- experiments. The asymmetry arises from the interference between the electromagnetic and weak interaction and depends on the weak axial-vector coupling of the electron and muon

$$A_{\mu\mu} \approx 4 \chi g_A^e \cdot g_A^\mu \quad (13)$$

The GSW-model predicts a negative asymmetry because g_A^e is equal to g_A^μ and χ is negative. This means that there are more $\mu^+\mu^-$ events with the μ^- in the backward hemisphere than events with the μ^- in the forward hemisphere.

To measure the asymmetry one needs to determine the direction and the charge of the muons. The asymmetry can be measured very precisely, because it is a relative measurement, independent of the luminosity measurement. It is insensitive to errors in the acceptance and reconstruction efficiency as long as the acceptance is the same for positive and negative muons. For this reason, the experiments are able to limit the systematic error of the asymmetry to $\pm 1\%$. In addition, MARK-J and MAC took equal amounts of data with positive and negative magnet polarity. The addition of both data sets effectively cancels all systematic errors, which relate to the charge measurement, and leaves no doubt that the systematic error is much smaller than 1%.

Figure 5 shows the angular distribution measured by the MARK II

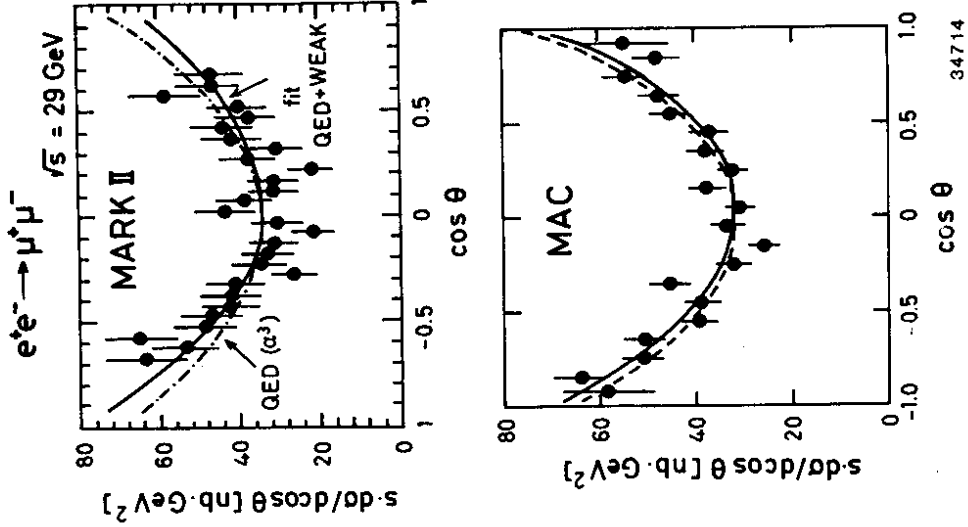


Fig. 5
Angular distribution
of the reaction
 $e^+e^- \rightarrow \mu^+\mu^-$ measured
by the MAC and
MARK II experiments
at PEP. The dashed
line is the predict-
ion of QED. The
solid line is the
best fit to the
electro-weak cross
section. Both
curves include QED
radiative correct-
ions to order α^3 .

and MAC detector at PEP. These measurements are not corrected for QED radiative effects and thus are compared with the QED prediction including corrections to order α^3 . The weak interaction should increase the cross section in the backward hemisphere (negative $\cos\theta$) and decrease the cross section in the forward hemisphere. We cannot detect a statistically significant asymmetry in these measurements at 29 GeV. Turning to the measurements at PETRA at $\sqrt{s} \approx 34.5$ GeV (Fig. 6), we see a clear and very significant negative asymmetry in the angular distribution measured by JADE, MARK-J and TASSO. This is mainly due to the higher c.m. energy, which increases the asymmetry by a factor 1.5, and due to the higher integrated luminosity reached by the PETRA storage ring. The measured values in Fig. 6 are corrected for QED radiative effects to order α^3 . Therefore, the data are compared to a $1 + \cos^2\theta$ distribution, predicted from lowest order QED (dashed line) and to a fit which includes an additional $\cos\theta$ terms as predicted by the weak interaction.

Before we discuss the significance of these measurements, we should be more explicit about radiative corrections. Pure QED also produces a forward backward asymmetry, for example, through the interference of the one and two photon exchange graphs.

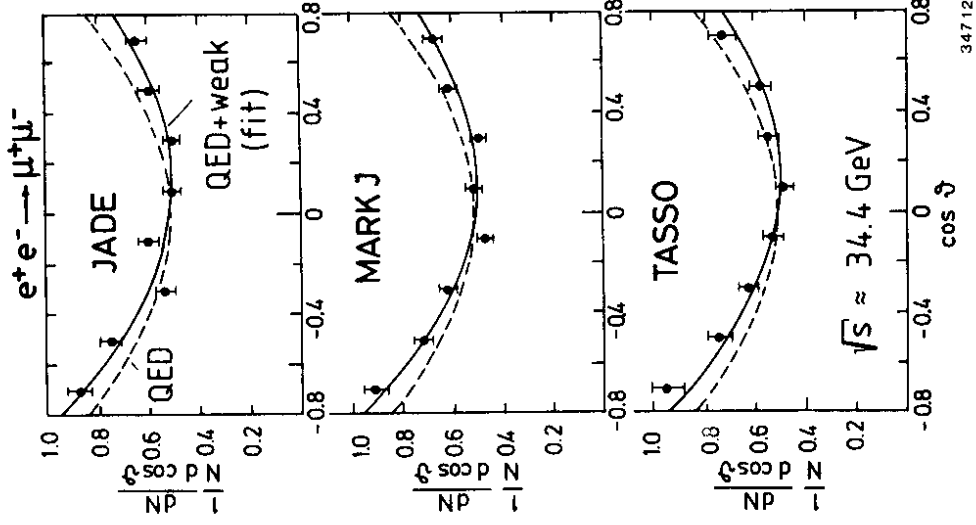
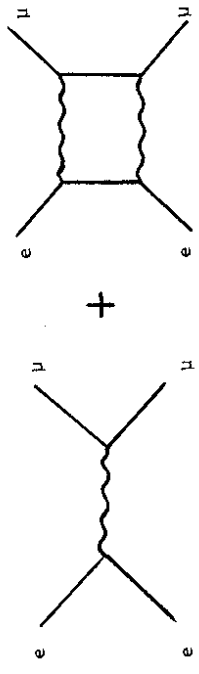


Fig. 6
Angular distribution
of the reaction
 $e^+e^- \rightarrow \mu^+\mu^-$
measured
by the PETRA exper-
iments JADE, MARK-J
and TASSO. The data
are corrected for
QED radiative
effects up to order
 α^3 . The dashed line
indicates the lowest
order QED prediction
of $(1-\cos^2\theta)$. The
solid line is a fit
to the data using
the electroweak cross
section, given by(6).

34712

The QED asymmetry is calculated by a Monte Carlo program from Berend and Kleiss (15). It is found to be $+1.5\%$ for $|\cos\theta| \leq 0.8$ if one applies an acollinearity cut of $\xi < 10^\circ$ and a cut on the muon momentum of $p_\mu > 1/2 p_{beam}$. In order to compare the measurements with the lowest order electroweak formula (10) one usually subtracts the QED asymmetry from the observed asymmetry

$$A_{\text{weak}} = A_{\text{observed}} - A_{\text{QED}} \quad (14)$$

This correction to the asymmetry is incomplete, because we should apply radiative corrections for QED and weak interactions.

A Monte Carlo program (17) which includes first order QED corrections and a large part of the weak corrections, gives an asymmetry of $A_{\text{weak}} = (-8.6 \pm 0.2)\%$ at $\sqrt{s} = 34.5 \text{ GeV}$. Since this value includes the correction from (14) it should be compared to the lowest order electroweak asymmetry of -9.4% , obtained from (6). Whether the difference between both values shows the presence of weak radiative corrections is unclear. A simpler explanation could be that the c.m. energy squared is reduced by initial state bremsstrahlung, which creates a corresponding reduction of the asymmetry, because the asymmetry is approximately proportional to s . However, until we find a clear explanation for this difference we use formula (6) to calculate the expected asymmetry and neglect the results of the Monte Carlo calculation. A better understanding of electroweak radiative corrections is urgently needed. Otherwise we will soon have the situation that the error on the theoretical prediction is of the same size as the error on the measured asymmetry.

Table II summarizes the high energy measurements of the asymmetry.

Only statistical errors are given with the measured asymmetries. The systematic errors are estimated to be smaller than 1% and are included in the combined results. The asymmetries in Table II are obtained from a fit of (6) to the measured angular distribution after it is corrected for radiative effects of QED to order α^3 . The parameters of the fit are $R_{\mu\mu}$ and the coefficient B of the $\cos\theta$ term of expression (6). The asymmetry is calculated from the ratio of B to $R_{\mu\mu}$.

$$A_{\mu\mu} = \frac{3}{8} \frac{B}{R_{\mu\mu}} \quad (15)$$

In this way one effectively extrapolates the angular distribution to $\cos\theta = 1$ and has the possibility of comparing the measured asymmetries directly to values calculated from the lowest order electroweak prediction (10).

TABLE II

Experiment	\sqrt{s} (GeV)	RESULTS FROM PEP AND PETRA ON THE ASYMMETRY OF $e^+ e^- \rightarrow \mu^+ \mu^-$	
		Measured $A_{\mu\mu}$ in %	Expected in GSW for $\sin^2 \theta_W = 0.23$ in Z
MAC	29	-4.4 \pm 2.4	-6.3
MARK II	29	-9.6 \pm 4.5	-6.3
PEP Results combined		-5.6 \pm 2.3	-6.3
CELLO	34.2	-6.4 \pm 6.4	-9.1
JADE	34.2	-10.8 \pm 2.2	-9.2
MARK-J	34.6	-10.4 \pm 2.1	-9.4
TASSO	34.4	-10.4 \pm 2.3	-9.3
PETRA Results combined	34.4	-10.4 \pm 1.4	-9.3 for $m_Z = 90 \text{ GeV}$ -7.9 for $m_Z = \infty$

All measurements agree well with the prediction of the GSW-theory for $\sin^2 \theta_W \approx 0.23$ which gives $g_A^{\mu} = g_A^e = -1/2$, $\delta_V \approx 0$ and $\delta_V \approx 90 \text{ GeV}$.

The asymmetry depends mainly on the product $g_A^e \cdot g_A^\mu$ and the Z^0 mass. If we include a systematic error of 1% on the asymmetry of each experiment, we can draw the following conclusion from Table III.

- 1) If we set $m_Z = 90$ GeV, we find

$$g_A^e \cdot g_A^\mu = 0.274 \pm 0.035$$

If we insert $g_A^e = -0.530 \pm 0.035$ from νe -scattering, we determine the axial-vector coupling of the muon

$$g_A^\mu = T_{3L} - T_{3R} = -0.52 \pm 0.10$$

The value is in perfect agreement with the assumption that the left-handed muon is the lower member of a weak iso-doublet and that the right-handed muon is in a weak iso-singlet. If we assume $T_{3L} = -1/2$, then we obtain $T_{3R} = 0.02 \pm 0.10$. Comparing g_A^e with g_A^μ we get an impressive confirmation of the $u-e$

universality in the weak interaction.

- 2) Alternatively, we can determine the Z^0 mass, $m_Z = 72^{+36}_{-10}$ GeV, if we assume $e-\mu$ universality and $g_A^2 = 1/4$ and $g_Y^2 \sim 0$. The one standard deviation error is somewhat misleading, because the upper 95% confidence limit extends to an infinite mass. However, a firm lower limit can be put on the Z^0 mass, which is 56 GeV with 95% confidence.

Figure 7 summarizes all existing measurements on this asymmetry.

The low energy points are from PETRA and from SPEAR⁽¹⁸⁾. We observe a clear dependence on the c.m. energy s as predicted for an electro-weak interference. The effect of a Z^0 propagator with a Z^0 mass of

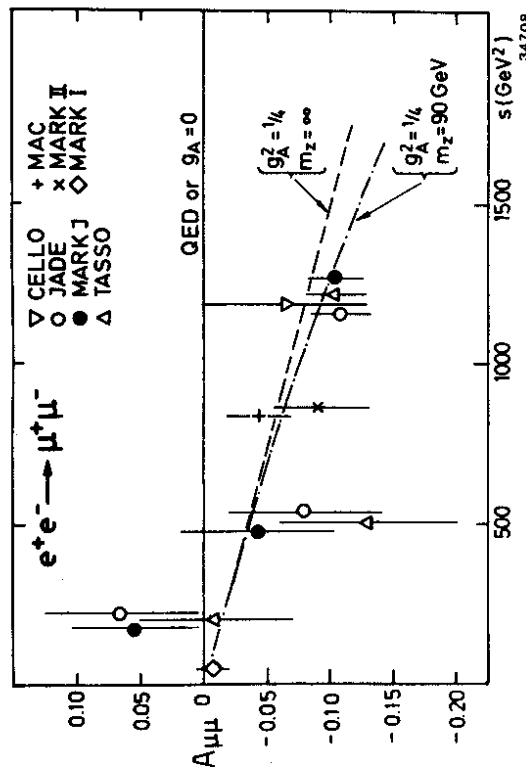


Fig. 7 Measurements of the forward backward asymmetry of the reaction $e^+ e^- \rightarrow \mu^+ \mu^-$ as a function of the c.m. energy squared. The data are compared to the predictions of the electroweak theory with $g_A^2 = 1/4$ for a pointlike four-fermion coupling, i.e. $m_Z = \infty$ (dashed line) and for $m_Z = 90$ GeV (dashed-dotted line). Since the measurements are corrected for radiative effects, pure QED or an electroweak theory with $g_A = 0$ predicts no asymmetry.

90 GeV cannot yet be distinguished from that of a point-like four fermion coupling ($m_Z = \infty$). However, at the end of 1982 PETRA will begin operating at an energy of 40 GeV ($s=1600$ GeV 2), where the effects of the Z^0 propagator are about twice that at $s=1200$ GeV 2 . With an equal amount of data at 40 GeV, we should be able to give an interesting lower and upper bound for the Z^0 mass.

VII. $e^+e^- \rightarrow \tau^+\tau^-$: CROSS SECTION AND BRANCHING RATIOS

We first discuss the measurement of the cross section $\sigma_{\tau\tau}$. Tau leptons are recognized by their characteristic decays, either into lepton and neutrinos or into hadrons (low multiplicity) and a neutrino. The branching fractions of tau-leptons which are accepted by a given detector range between 28% for MARK-J and TASSO to 94% for CELLO and MAC, because the experiments use different decay modes to select tau events. The systematic error on the cross section is generally larger than for $\sigma_{\mu\mu}$ and ranges between 10% and 20%, if one includes the errors of the branching ratios. The reader is referred to the original publications for a detailed description of the selection and measurement of tau events (10-13),(19,20)

The measured cross sections are corrected for acceptance and for QED radiative effects to order a^3 so that they can be compared directly to the lowest order QED cross section. If we plot the ratio $R_{\tau\tau}$ of the tau cross section divided by the pointlike cross section we remove the $1/s$ dependence of the cross section and simplify the comparison of the measurements to the QED prediction, which is $R_{\tau\tau}=1$.

Figure 8 shows the measured values for $R_{\tau\tau}$ as a function of s , which agree well with QED within the statistical and systematic errors. The effect of the weak interaction on $R_{\tau\tau}$ can still be neglected within measurement errors because it is proportional to $\frac{e^{\tau}}{g_V g_Y}$, where at least the vector coupling of the electron is close to zero. Thus, from Fig. 8 we can draw the following conclusions.

- 1) The agreement of the tau cross section with the QED prediction leads to an upper limit for the cut-off parameter of $\Lambda \approx 120$ GeV with 95% confidence level. We conclude that the tau interacts as a pointlike lepton down to distances as small as 2.10^{-16} cm.
- 2) Alternatively, we assume the validity of QED and determine the branching ratios of tau decay modes which were used for the selection of $ee \rightarrow \tau\tau$. MAC(13), MARK-J(21), and PLUTO(22) measure the branching ratio of $\tau \rightarrow \mu\nu\nu$. Their results are listed in Table III together with a result from MARK II at SPEAR(22).

TABLE III
RESULTS ON THE BRANCHING RATIO FOR $\tau \rightarrow \mu\nu\nu$

Experiment	$B(\tau \rightarrow \mu\nu\nu)$ in %
MAC	17.6 ± 1.5 ± 1.0
MARK-J	16.3 ± 1.6
PLUTO	17.8 ± 2.0 ± 1.0
MARK II (SPEAR)	17.1 ± 0.6 ± 1.0
AVERAGE	17.1 ± 0.8

Tau leptons can also be recognized by their decay into charged hadrons of low multiplicity. Denote by B_1 , B_3 and B_5 the branching

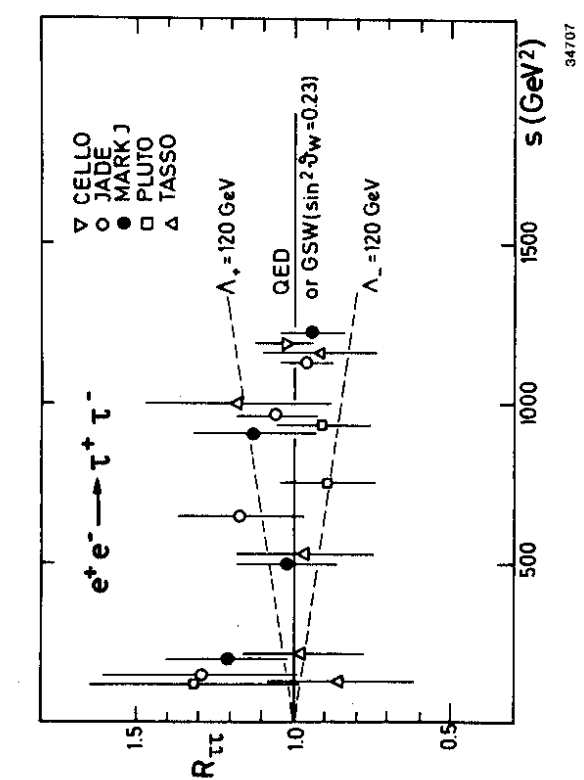


Fig. 8 Measurements of $R_{\tau\tau}$ at different c.m. energies squared. The

solid line shows the prediction of pure QED which coincides with the prediction of the GSW-theory for $\sin^2 \theta_W = 0.23$.

Also indicated are the deviations expected if the cut-off parameter Λ_+ would be 120 GeV.

VIII. $e^+ e^- \rightarrow \tau^+ \tau^-$: ASYMMETRY

The angular distribution of tau leptons should show a forward backward asymmetry proportional to $g_A^e g_A^\tau$ analogous to the reaction $ee \rightarrow \mu\mu$. If $g_A^e = g_A^\tau = -1/2$ we expect an asymmetry of -9.7% at 35 GeV. This means that negative taus go more frequently in the direction of the positron beam and positive taus tend to follow the electron beam. The charge of the tau lepton is easily determined from the sum of the charges of its decay products. Most of the experiments do not detect all decay modes and have therefore a smaller number of events than in the reaction $ee \rightarrow \mu\mu$, with attendant larger statistical errors.

ratios of taus into one, three and five charged particles and additional neutral particles. Table IV shows the branching ratios which have been measured by CELLO(19), MAC(13), MARK II(20), and TASSO(23). The branching ratios are constrained by requiring $B_1 + B_3 + B_5 = 1$, since there must be at least one charged particle in the decay of a tau lepton.

TABLE IV

BRANCHING RATIOS B_n OF THE TAU LEPTON INTO $n = 1, 3$ AND 5 CHARGED PARTICLES AND ADDITIONAL NEUTRALS

Experiment	B_1 in %	B_3 in %	B_5 in %
CELLO	84.0±2.0	15.0±2.0	1.0±0.4
MAC	84.6±0.7±1.0	15.3±0.7±1.0	< 0.7%
MARK II	86.0±3.0±1.0	14.0±3.0±1.0	< 0.7% 95%
TASSO	76.0±6.0	24.0±6.0	< 6%
Average	84.3±1.0	15.3±1.0	

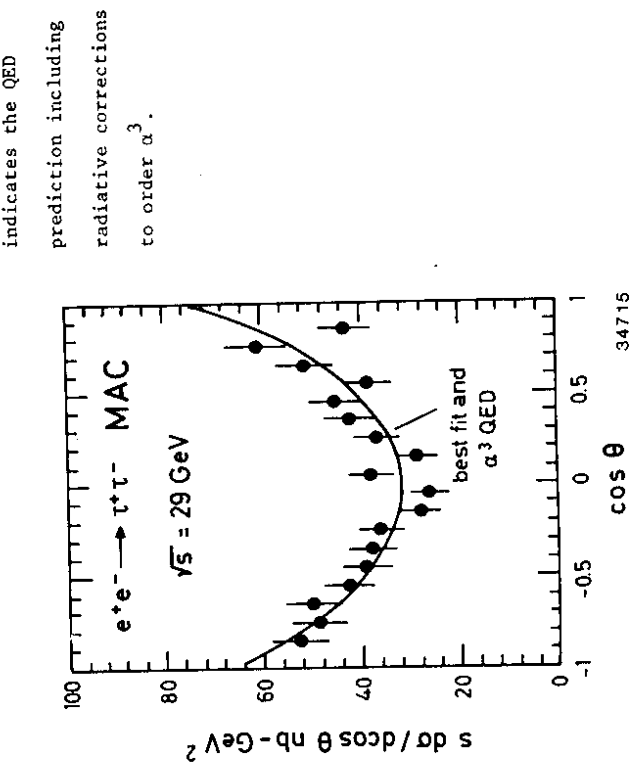
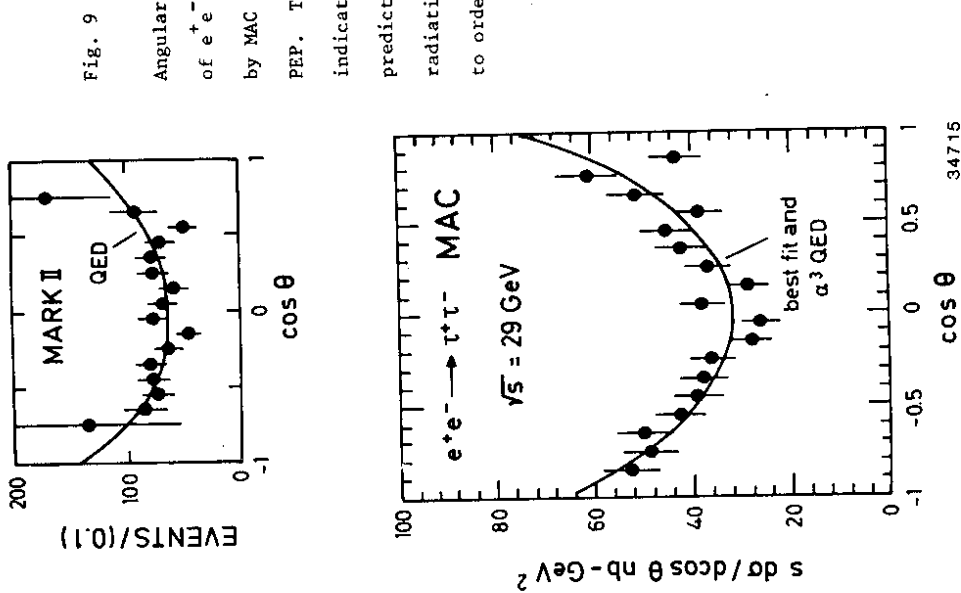
Figure 9 shows the angular distribution measured by MAC and MARK II at $\sqrt{s} = 29$ GeV. The prediction from QED including α^3 QED correction coincides with the best fit, which includes the weak interaction. This means that, within measurement errors a weak interaction asymmetry is not observed. However, we should not forget that the expected asymmetry at $\sqrt{s} = 29$ GeV is small, only -6.3%. The angular distributions measured by PETRA experiments at $\sqrt{s} \approx 34.4$ GeV are plotted in Fig. 10. The angular distributions are corrected for radiative effects of order α^3 and should therefore be compared with the lowest order QED or electroweak prediction. All four measurements depart slightly from the symmetric $(1+\cos\theta)^2$ distribution predicted by pure QED and prefer a small negative asymmetry. The angular distributions of Fig. 9 and Fig. 10 are fitted with the electroweak prediction in the form of expression (6) by varying $R_{\tau\tau}$ and B the coefficient of the asymmetric term of the cross section. The forward backward asymmetry of taus is calculated by

$$A_{\tau\tau} = \frac{B}{R_{\tau\tau}} \quad (16)$$

which can be compared to the electroweak prediction

$$A_{\tau\tau} = 4Xg_A^e g_A^\tau \quad (17)$$

The tau asymmetries measured at PEP and PETRA are listed in Table V. The measurements have a systematic error of 1% to 2% in addition to the statistical error given in Table V.



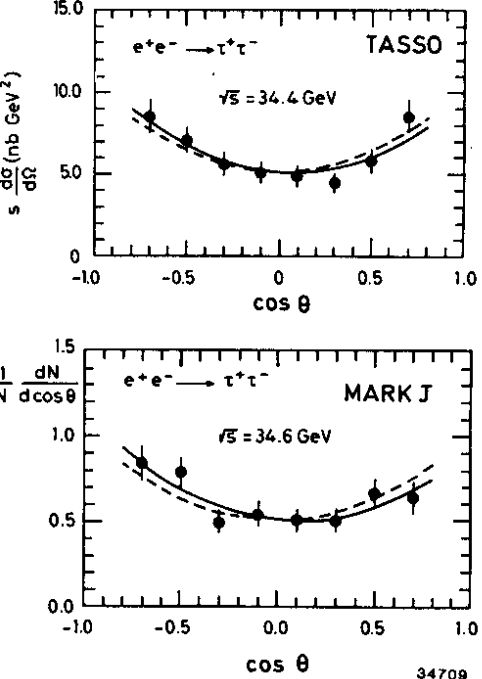
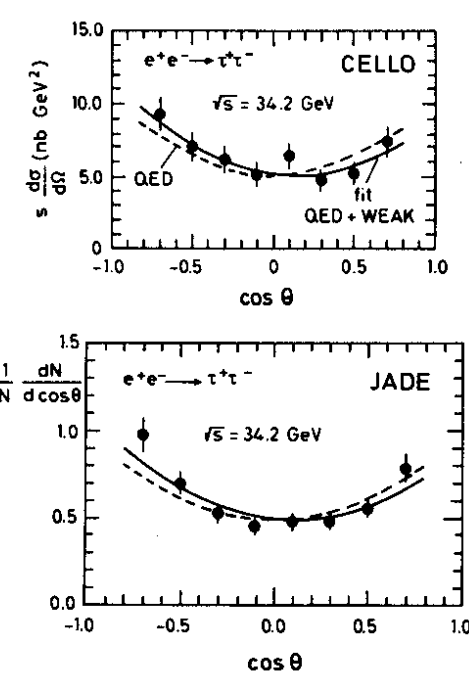


Fig. 10
Angular distribution of $e^+e^- \rightarrow \tau^+\tau^-$ measured by CELLO, TASSO, JADE and MARK-J at PETRA.
The data are corrected for QED radiative effects to order α^3 . The dashed line is the lowest order QED prediction of the form $(1+\cos^2\theta)$.

The solid line is a fit to the data, which includes weak interaction in the form of expression (6).

TABLE V
RESULTS FROM PEP AND PETRA ON THE ASYMMETRY IN THE REACTION $e^+e^- \rightarrow \tau^+\tau^-$

Experiment	\sqrt{s} GeV	$A_{\tau\tau}$ in %	Expected in GSW for $\sin^2\theta_W = 0.23$
MAC	29	-1.3±2.9	-6.3
MARK II	29	-3.2±5.0	-5.0 ($ \cos\theta <0.7$)
PEP Combined	29	-1.7±2.5	-6.0
CELLO	34.2	-10.3±5.2	-9.2
JADE (prelim)	34.2	-7.9±3.9	-9.2
MARK-J	34.6	-8.4±4.4	-9.4
TASSO	34.4	-5.4±4.5	-9.3
PETRA Combined	34.4	-7.9±2.2	-9.3

The experiments at PETRA find a negative asymmetry with a typical significance of two standard deviations. Their combined value of $(-7.9\pm2.2)\%$ is the first significant observation of an electroweak interference associated with tau leptons. It agrees well with the expected value of -9.3% and $e-\mu-\tau$ universality in weak interactions.

The asymmetry of $ee \rightarrow \tau\tau$ measures the product $g_A^e g_A^\tau$. By combining all PEP and PETRA measurements we find (for $m_Z = 90$ GeV)

$$g_A^e \cdot g_A^\tau = 0.18 \pm 0.05.$$

If we insert $g_A^e = 0.530 \pm 0.035$ from νe -scattering we determine the axial vector coupling of the tau lepton

$$g_A^\tau = T_{3L} - T_{3R} = -0.34 \pm 0.12.$$

This value is consistent with the assumption that the left-handed tau is the lower member of a weak iso-doublet and the right-handed

tau is in a weak iso-singlet.

IX. COMBINED RESULTS FROM LEPTONIC REACTIONS

We now assume $e-\mu-\tau$ universality and attempt a combined fit to the leptonic reactions $e^+e^- \rightarrow \ell^+\ell^-$, where ℓ is an electron, muon or tau lepton. We can either assume the validity of the GSW theory and determine $\sin^2\theta_W$ or allow an independent variation of the vector and axial-vector coupling. In the second case, we should also vary the Z^0 mass, but the data are not yet accurate enough to determine the Z^0 mass. We therefore give the results of g_V^2 and g_A^2 for a Z^0 mass of 90 GeV. Table VI lists the results from different experiments. Both statistical and systematic errors are included.

We now assume $e-\mu-\tau$ universality and attempt a combined fit to the leptonic reactions $e^+e^- \rightarrow \ell^+\ell^-$, where ℓ is an electron, muon or tau lepton. We can either assume the validity of the GSW theory and determine $\sin^2\theta_W$ or allow an independent variation of the vector and axial-vector coupling. In the second case, we should also vary the Z^0 mass, but the data are not yet accurate enough to determine the Z^0 mass. We therefore give the results of g_V^2 and g_A^2 for a Z^0 mass of 90 GeV. Table VI lists the results from different experiments. Both statistical and systematic errors are included.

TABLE VI

RESULTS OF A COMBINED FIT TO LEPTONIC REACTIONS. THE THEORETICAL PREDICTION OF THE GSW-THEORY ARE OBTAINED WITH $\sin^2\theta_W = 0.23 \pm 0.01$ AS MEASURED BY νN AND $\bar{\nu} N$ SCATTERING EXPERIMENTS

Experiment	Reaction Used	g_V^2	g_A^2	$\sin^2\theta_W$
MAC	$ee, \mu\mu, \tau\tau$	<0.11(95% C.L.)	$0.16^{+0.08}_{-0.06}$	0.24 ± 0.10
MARK II	$ee, \nu\nu$	0.05 ± 0.10	0.24 ± 0.16	
CELLO	$ee, \mu\mu, \tau\tau$	-0.03 ± 0.08	0.31 ± 0.12	$0.21^{+0.14}_{-0.09}$
JADE	$\mu\mu$	0.05 ± 0.08	0.29 ± 0.06	
MARK-J	$ee, \mu\mu, \tau\tau$	-0.02 ± 0.05	0.28 ± 0.06	0.26 ± 0.09
TASSO	$ee, \mu\mu, \tau\tau$	-0.04 ± 0.06	0.26 ± 0.07	0.27 ± 0.07
Combined Data on $ee, \nu\nu$ From JADE, MARK-J, TASSO	0.01 ± 0.03	0.28 ± 0.04	0.27 ± 0.07	
νe -Scattering	$0.00^{+0.01}_{-0}$	0.28 ± 0.04	0.27 ± 0.03	
GSW Theory	0.04	0.25	0.23 ± 0.01	

The data of JADE, MARK-J and TASSO on the reactions $ee \rightarrow ee$ and $ee \rightarrow \mu\mu$ are also combined in a fit, which includes the normalization error and the systematic error of each experiment. All results given in Table VI agree very well with the predictions of the GSW-theory for $\sin^2\theta_W = 0.23 \pm 0.01$, as measured by νN and $\bar{\nu} N$ scattering (2) and so confirms the validity of the GSW-theory at high q^2 and s up to 1200 GeV^2 .

Fig. 11 displays the values for $\sin^2\theta_W$ measured in different reactions and indicates the typical momentum transfer. It is very impressive to see that one parameter, $\sin^2\theta_W \approx 0.23$, describes all of these reactions.

It should also be noted that the results of Table VI are obtained from purely leptonic e^+e^- reactions and can therefore be compared to measurements of neutrino electron scattering. The results from both types of experiments have a similar precision and show an excellent agreement. A comparison with the neutrino electron experiments can also be done in more detail, if one displays the results in the (g_V, g_A) -plane (Fig. 12). The allowed region for g_V and g_A has a four-fold symmetry because e^+e^- experiments measure the square of the coupling constants. Neutrino scattering alone limits the values to two regions, a vector-like and a axial-vector-like solution. To resolve this ambiguity one previously had to consider lepton-hadron scattering with the inherent complications of hadronic targets. Now a unique solution can be determined from purely leptonic reactions.

To come to this conclusion we have assumed in expression (1) that $h_{VV} = g_V^2$ and $h_{AA} = g_A^2$ or equivalently $c_{V_V} = 1$. Sakurai has proposed to compare the ratios h_{VV}/h_{AA} and g_V^2/g_A^2 which are independent of the

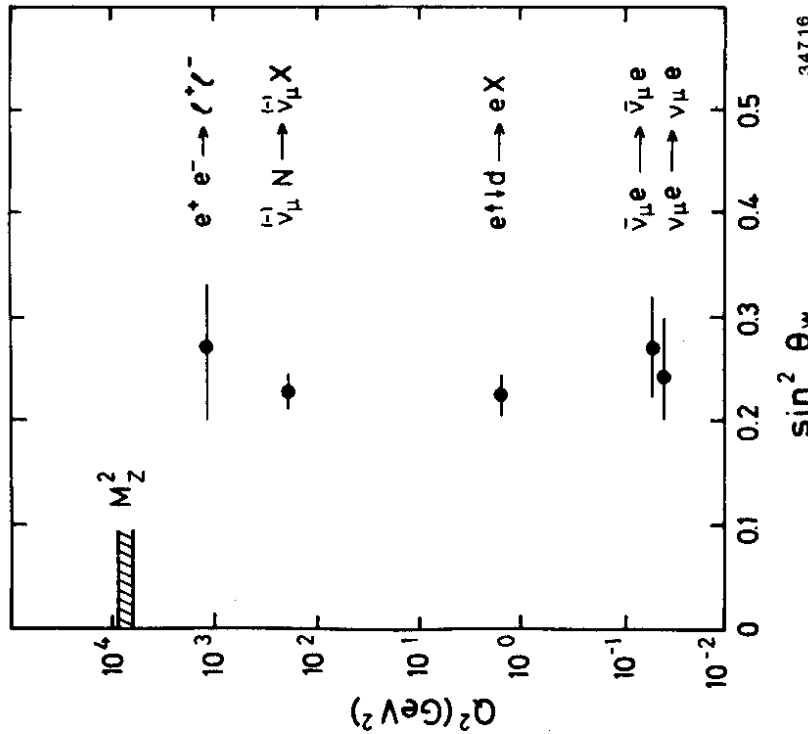


Fig. 11 The measurements of $\sin^2 \theta_W$ from different reactions are plotted as a function of the momentum transfer squared. Note that the Q^2 is mainly time-like in $e^+ e^- \rightarrow l^+ l^-$, in contrast to the other reactions.

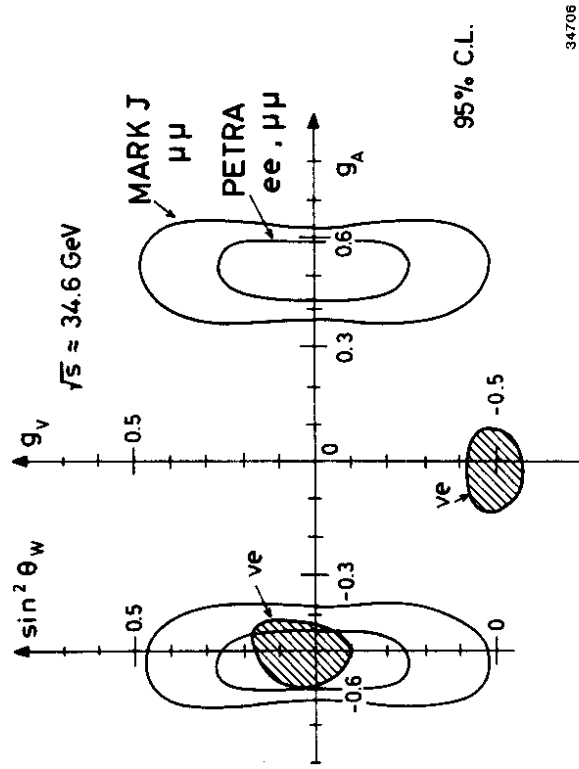


Fig. 12 Allowed regions (95% C.L.) for the vector and axial vector coupling of leptons determined by neutrino electron scattering (shaded area) and by $e^+ e^-$ experiments (unshaded regions). The contour of the MARK-J experiment results only on the measurement of $e^+ e^- \rightarrow \mu^+ \mu^-$, while the contour of the PETRA experiments is obtained from a combined fit of the reactions $e^+ e^- \rightarrow e^+ e^-$ and $e^+ e^- \rightarrow \mu^+ \mu^-$. The vector-like solution from νe scattering is clearly excluded, while the axial vector-like solution predicted by the GSW theory for $\sin^2 \theta_W = 0.23$ is in very good agreement with the measurements of $e^+ e^- \rightarrow \nu \bar{\nu}$.

value of c_V , to exclude one solution (24). From the results of e^+e^- experiments listed in Table IV we find

$$\frac{g_V^2}{g_A^2} = \frac{h_{VV}}{h_{AA}} < 0.27 \text{ with 95% confidence.}$$

This limit clearly excludes the vector-like solution of the neutrino electron scattering data on a more general ground, namely in the framework of models with a single Z^0 .

X. MULTI-BOSON MODELS

Now we abandon the restriction of one neutral gauge boson and consider the gauge groups $SU(2) \times U(1) \times G$. These models (25, 26) have an effective neutral current lagrangian, which becomes in the low q^2 limit

$$L_{\text{eff}}^{\text{NC}} = -\frac{4G_F}{\sqrt{2}} \left[(j_\mu^3 - \sin^2 \theta_W j_\mu^{\text{em}})^2 + C (j_\mu^{\text{em}})^2 \right] \quad (18)$$

It differs from $SU(2) \times U(1)$ by a term proportional to the square of the electromagnetic current which is parity conserving and which is therefore invisible in the neutrino experiments and in polarized electron-deuteron scattering. However, it modifies the vector coupling and

h_{VV} , previously given by (5), becomes

$$h_{VV} = \frac{1}{4} (1 - 4 \sin^2 \theta_W)^2 + 4C \quad (19)$$

To reproduce the low energy neutrino and electron-deuteron results we

use $\sin^2 \theta_W = 0.23$ and determine a limit on C . Experiments at PETRA find the upper limits (95% C.L. listed in Table VII).

TABLE VII
UPPER LIMITS FOR THE PARAMETER C WITH 95% CONFIDENCE

	C
CELLO	0.031
JADE	0.039
MARK-J	0.021
TASSO	0.018
Combined	0.015

The parameter C is positive and a function of the couplings and masses of the Z^0 bosons. The mass limits for models with two neutral bosons, where G is a $U(1)$ or a $SU(2)$ group (26), are shown in Fig. 13. We see that the neutral boson masses are limited to a small region, where one of the Z^0 's has a mass near to 90 GeV as predicted by the standard $SU(2)_L \times U(1)$ theory.

XI. HADRON PRODUCTION $e^+e^- \rightarrow q\bar{q}$

Hadronic production in e^+e^- annihilation is well described by the pair production of spin $-\frac{1}{2}$ quarks, which subsequently fragment into jets of hadrons. The cross section for the production of a quark-antiquark pair of flavor f can be obtained from formula (6) by replacing the electric and weak charges of the muon by Q_f and g_V^f, g_A^f , respectively, and multiplying the result by a factor three for the color degrees of freedom. The relative cross section R_f is then given by (27)

$$R_f = 3(O_f^2 - 2Q_f g_V^e g_V^f + \chi^2 [(g_V^e)^2 + (g_A^f)^2] [(g_V^f)^2 + (g_A^e)^2]) \quad (20)$$

The vector and axial vector couplings of the quark are determined in the standard $SU(2)_L \times U(1)$ model by the third component of the weak isospin and by the weak mixing angle.

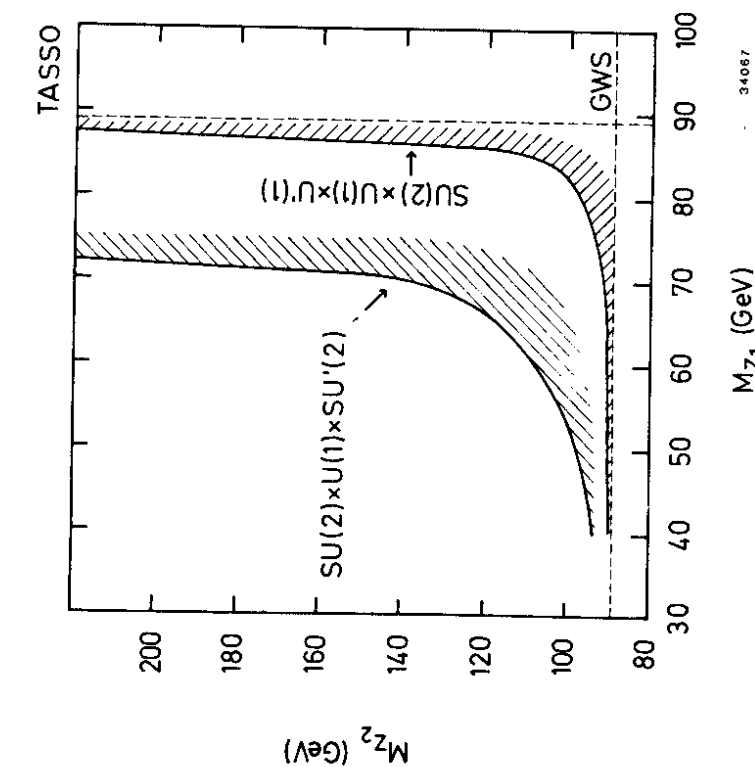


Fig. 13 Limits on the Z^0 masses for models with two Z^0 bosons.

The allowed masses of Z_1 and Z_2 are confined to the region (partially shaded) between the solid curve and the dashed lines.

If we arrange the left-handed quarks in weak iso-doublets $(\begin{smallmatrix} u \\ d \end{smallmatrix})$, $(\begin{smallmatrix} c \\ s \end{smallmatrix})$, $(\begin{smallmatrix} t \\ b \end{smallmatrix})$, we assign $T_{3L} = +\frac{1}{2}$ to the quarks u , c and t , and $T_{3L} = -\frac{1}{2}$ to the quarks d , s and b .

The total hadronic cross section is the sum of R_f over the five quark flavors u , d , s , c , b multiplied by a QCD correction

$$R = \sum_f R_f (1 + \frac{\alpha_s}{\pi} + \dots) \quad (22)$$

The variation of R with $\sin^2 \theta_w$ is shown in Fig. 14. At first one might think that the effect is too small to be observed, but the hadronic cross section increases by 11%, if $\sin^2 \theta_w$ changes from 0.10 to 0.30. This increase is still rather small in view of the systematic errors which range between 3% and 6% for different experiments. The largest contribution to the systematic error comes from an uncertainty in the absolute normalization of the cross section.

If there is a systematic error, it should be independent of the c.m. energy, whereas the contribution of the weak interaction to the hadronic cross section increases with the square of the c.m. energy. Thus, by measuring the energy dependence of R a determination of $\sin^2 \theta_w$ can be made. Measurements of R between 12 and 36 GeV have been obtained at PETRA (Fig. 15). The data have been fitted using equation (22) but allowing the overall normalization to vary within the errors. The strong coupling constant was taken as $\alpha_s = 0.17$ by MARK-J and TASSO and as 0.18 by JADE. The values of $\sin^2 \theta_w$ are insensitive to the value of α_s , because they are determined from the energy dependence of R , not from its magnitude. Table VII summarizes

the values (19, 28, 29) of $\sin^2 \theta_w$ and that of $\langle R \rangle$, which is averaged over the energy range between 14 GeV and 36 GeV.

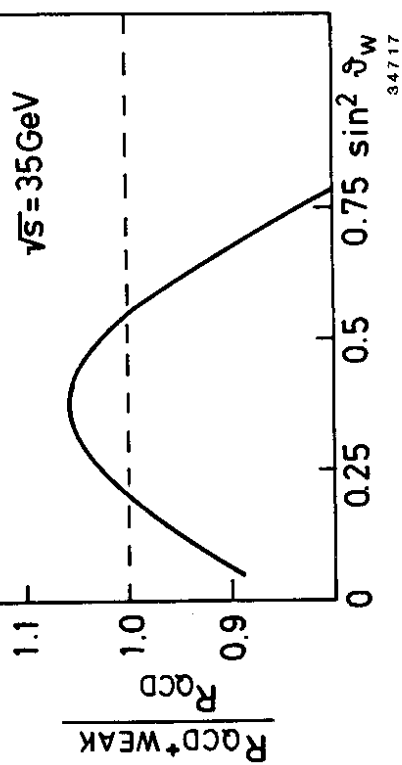


Fig. 14 Dependence of the hadronic cross section on $\sin^2 \theta_w$.
 $R_{QCD+WEAK}$ is calculated with formula (22) including the weak interaction, while R_{QCD} is calculated without the weak interaction, i.e. with $g_V = g_A = 0$.

TABLE VII
VALUES OF $\sin^2 \theta_w$ AND OF $\langle R \rangle$

Experiment	$\langle R \rangle$	$\sin^2 \theta_w$ from $e^+ e^- \rightarrow q\bar{q}$	$\sin^2 \theta_w$ from $e^+ e^- \rightarrow q\bar{q}$ and $e^+ e^- \rightarrow \ell^+ \ell^-$
JADE	$3.93 \pm 0.03 \pm 0.09$	0.25 ± 0.05	-
MARK-J	$3.84 \pm 0.05 \pm 0.22$	0.44 ± 0.11	0.30 ± 0.06
TASSO	$4.01 \pm 0.03 \pm 0.20$	$0.40 \pm 0.15 \pm 0.02$	-

The large spread of values of $\sin^2 \theta_w$ and its error is explained by the fact that the χ^2 curves of the fits are rather flat for $0.25 < \sin^2 \theta_w < 0.55$. Figure 14 shows that the contribution of the weak interaction is symmetric around $\sin^2 \theta_w \approx 0.38$, with generally two solutions for $\sin^2 \theta_w$. Additional measurements are needed to exclude one of these. Because the hadronic cross section depends on the product of the quark and electron couplings, the MARK-J group prefers to quote $\sin^2 \theta_w$ determined from a combined fit of hadronic and leptonic reactions. This value is also given in Table VII. Clearly, the precision of these measurements of $\sin^2 \theta_w$ cannot compete with the neutrino-nucleon and electron-deuteron measurements, but the results give support to the validity of the GSW-theory and its applicability in the region of time-like q^2 up to 1200 GeV 2 .

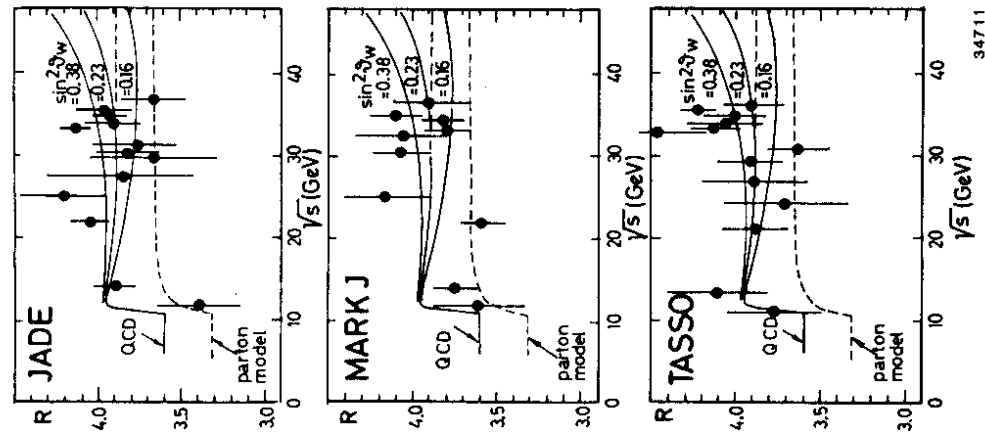


Fig. 15

XII. FORWARD-BACKWARD ASYMMETRY IN $e^+ e^- \rightarrow \bar{q}q$

The measurement of the angular distribution of jets in the reaction $e^+ e^- \rightarrow \bar{q}q$ offers the possibility of observing the forward backward asymmetry of quarks and of determining the axial vector coupling of quarks on the condition that we find a method of distinguishing quark jets from antiquark jets. The situation is completely analogous to that of the muon asymmetry, where we must distinguish a μ^- from its antiparticle, μ^+ . The methods of separating quarks from antiquarks will be described later in this chapter. For the moment we assume that we are able to do so and discuss the angular distribution and asymmetry of quarks. The main terms of the angular distribution of a quark of flavor f can be written

$$\frac{2s}{\pi\alpha} \frac{d\sigma}{d\cos\theta} \approx 3Q_f^2 (1+\cos^2\theta) - 12Q_f g_A^e g_A^f \cos\theta + \dots \quad (23)$$

where θ is the angle of the quark, not the antiquark, with respect to the electron beam direction. We see from (23) that the QED contribution to the cross section is proportional to Q_f^2 , while the electro-weak interference term is proportional to Q_f . Because the asymmetry depends mainly on the ratio of the interference term to the QED term, it is increased by a factor $1/Q_f$ and we find

$$A_F \approx -\frac{3}{2} \times \frac{1}{Q_f} \frac{g_A^e g_A^f}{g_F^e g_F^f} \quad (24)$$

The asymmetry A_F measures the axial-vector coupling of a quark divided by its charge. The axial-vector coupling depends on the third component of the weak isospin of left handed and of right-handed

quark fields.

$$g_A^f = T_{3L} - T_{3R} \quad (25)$$

Thus the asymmetry is sensitive to the multiplet structure of weak isospin. If we assume only left handed iso-doublers and right handed iso-singlet and arrange the left handed quarks in the following doublet structure

$$\begin{pmatrix} u \\ d \end{pmatrix} \begin{pmatrix} c \\ s \end{pmatrix} \begin{pmatrix} t_b \\ b \end{pmatrix}$$

we obtain

$$g_A^f = +\frac{1}{2} \text{ for } u, c, \text{ and } g_A^e = -\frac{1}{2} \text{ for } d, s, b.$$

Since the ratio g_A^f/Q in expression (24) is always positive and χ and g_A^e are negative, we should observe a negative asymmetry for all quark flavors. In addition, we find that the absolute value of the asymmetry is increased by a factor $1/Q_f$ compared to the muon asymmetry. If we include a correction due to the quark mass (30), we expect $A_c = -14\%$ and $A_b = -25\%$ at 34 GeV. At first sight, these high values appear easy to measure, but an analysis of the μ -inclusive events shows that the observed asymmetries are in fact very much smaller. This results from background and an incomplete separation of c - and b -quarks which we now explain in more detail.

The forward backward asymmetry of a quark flavor can only be measured when we are able to distinguish quarks from antiquarks. This means that we have to determine the quark flavor and the quark charge. In principle this can be achieved with a study of hadronic events which contain a "prompt" lepton (μ - or e -inclusive events) (31)



We call a lepton "prompt" when it appears to come from the interaction point where it originates from a semileptonic decay of a heavy quark produced in the $e^+ e^-$ reaction. More precisely, the heavy quark fragments into a short lived hadron of the same flavor whose decay is described in the spectator model as the decay of the heavy quark. The sign of the prompt lepton charge indicates the sign of the charge of the parent quark. Examples are



The cascade decay $b \rightarrow c \rightarrow \mu^+ X$ creates some charge confusion but the lepton spectrum is softer and so a cut on the lepton momentum should in principle eliminate a large number of these events. If we neglect this problem for a moment, we find that positive muons select c -quarks and b -antiquarks; negative muons select c -antiquarks and b -quarks. If we are not able to separate the quark flavors b and c , their asymmetry will partially cancel, because we add particle and antiparticle asymmetries. Therefore a good flavor separation is of major importance for this measurement.

Quark flavors can be selected with variables, which are sensitive to the quark mass. In our present understanding, we believe that b -quarks fragment into broader jets than c -quarks of the same momentum. Since thrust measures the width of a jet, it is a good candidate for a variable to separate bottom from charm. Other variables are the transverse momentum p_T of the prompt lepton with respect of the

thrust axis or the angle δ between the lepton direction and the thrust axis. MARK-J uses a cut $\cos\delta < 0.925$ and TASSO uses a cut $p_T > 1$ GeV to select b-decays (19, 32). A Monte Carlo calculation simulating these cuts predicts that 35% of the selected events are b-quarks. The remainder is background from c-decays, π^- and K-decay and from hadrons which penetrate the muon filter and are misidentified as muons (punch-through). Charm decays are selected with complementary cuts. Half of the events in this sample are c-decays, the remainder is again K- and \bar{K} -decay and punch through. The quark asymmetries computed from these samples are listed in Table VIII.

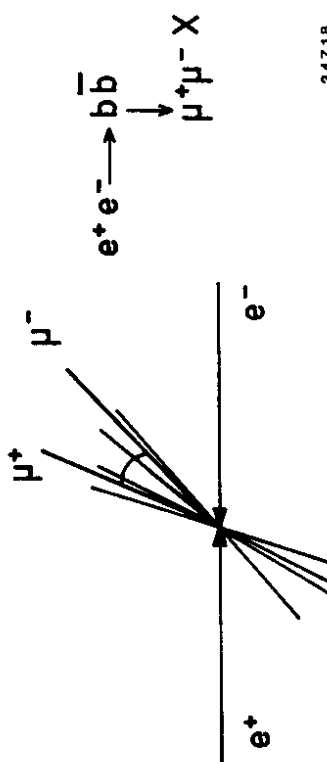


Fig. 16 Illustration of the signature of an event where one bottom quark decays via a flavor changing neutral current. A cut on the angle between the two muons eliminates background.

TABLE VIII

RESULTS OF FIRST ATTEMPTS TO MEASURE THE FORWARD-BACKWARD ASYMMETRY OF BOTTOM AND CHARM QUARKS AT 35 GEV. THE MEASURED AND EXPECTED VALUES INCLUDE THE EFFECTS OF BACKGROUND AND INCOMPLETE FLAVOR SELECTION

Experiment	Measured	Expected
MARK-J	$A_b = -(17 \pm 10)\%$	- 5%
TASSO	$A_b = -(20 \pm 10)\%$	- 8%
MARK-J	$A_c = -(7 \pm 5)\%$	- 4%

The results in Table VIII are very preliminary and only give an indication of the status of the analysis. Incomplete flavor separation and background strongly decrease the initially expected large asymmetries. We see from Table VIII that the expected bottom asymmetry is -5% to -8% instead of -25% which one calculates for a pure bottom sample. Clearly, the discrimination between bottom, charm, and the background level will need to be improved if significant

results are to be obtained. The statistical accuracy cannot be improved easily because these results are already based on a large amount of data. For example, the initial data sample of the MARK-J group contains 15,500 hadronic events from which 352 candidates of charm decays and 89 candidates of bottom decays are selected.

A different method for flavor tagging has been employed by TASSO (32). Charged D* mesons are reconstructed from the decay modes $D^{*+} \rightarrow D^0 \pi^+ \rightarrow K^- \pi^+ \pi^+$ and $D^{*+} \rightarrow K^- \pi^+ \pi^-$. The D* mesons are selected from the large number of $K\pi\pi$ combinations by a cut on the mass difference ΔM between the D* mass and the D⁰ mass. The events fulfilling the cut $142 < \Delta M < 148$ MeV show a D⁰ peak with 47 events. The background is estimated to be 11 events so that a signal of 36 charged D* mesons is detected. With these events the TASSO group finds a forward backward asymmetry of $A_C = -(35 \pm 14)\%$, where one expects -11% in the GSW model. Again, the number of events is too small to measure a statistically significant asymmetry. The hope is that with better mass resolution and with higher acceptance the statistical significance of this measurement will improve in the future.

its branching ratio(33)

$$B(\mu^+ \mu^- X) \geq 1\%$$

A search for this decay mode of the bottom quark has been made by CLEO at CESR and recently by MARK-J at PETRA. Here we will describe the analysis of the MARK-J group. Hadronic events with a $\mu^+ \mu^-$ pair in one jet are selected as illustrated in Fig. 16. If the muon pair originates from the decay of a b-quark, the angle between the two muons should be rather large due to the high mass of the b-quark.

A cut of $> 15^\circ$ is chosen for this angle. One candidate has been found in a sample of 28,400 hadronic events which contains 2,570 b \bar{b} events. However, one background event is also expected. The acceptance for this decay mode was calculated by a Monte Carlo program and found to be 7.1% which leads to a lower limit on the branching ratio determined by MARK-J.

$$B(b \rightarrow \mu^+ \mu^- X) < 0.6\% \text{ with } 90\% \text{ C.L.}$$

The CLEO group at CESR in similar analysis finds(34)

$$B(b \rightarrow \mu^+ \mu^- X) < 0.9\% \text{ with } 90\% \text{ C.L.}$$

We conclude from these results that the b-quark is a member of a weak iso-doublet and we should not give up searching for the top quark. It might turn out that we discover the existence of a top quark at PETRA in the year 1983 when energies up to 42 GeV become available.

XIII. FLAVOR CHANGING NEUTRAL CURRENTS

If the top quark does not exist and/or if the bottom quark is in a weak SU(2) singlet, flavor changing neutral currents would be expected in the b-decay. A good signature for this process is the decay $b \rightarrow \mu^+ \mu^- X$. Theoretical calculations give a lower limit for

CONCLUSIONS

- 1) In $e^+e^- \rightarrow \mu^+\mu^-$, JADE, MARK-J and TASSO have observed a statistically significant forward backward asymmetry $A_{\mu\bar{\mu}} = (-10.8 \pm 2.2)\%$, $(-10.4 \pm 2.1)\%$, $(-10.4 \pm 2.3)\%$ respectively. These values are in good agreement with the expectation of -9.3% from the GSW-model.
- 2) Leptonic reactions in e^+e^- experiments test the electroweak theories up to $s = 1200 \text{ GeV}^2$ and $q^2 \approx 1000 \text{ GeV}^2$. We find impressive agreement with the GSW model and determine $\sin^2\theta_W = 0.27 \pm 0.07$.
- 3) In a study of $e^+e^- \rightarrow$ hadrons first attempt have been made to measure the weak neutral current couplings of heavy quarks, but more statistics is needed in the case of D*-tagging and a better separation of bottom from charm quarks in ν -inclusive events is necessary in order to achieve significant results.
- 4) No flavor changing neutral currents have been observed $B(b \rightarrow \mu^+\mu^- X) < 0.6\%$ (90% C.L.)
- 5) Charged Higgs particles and technipions are excluded for masses between the tau mass and 13 GeV (19, 34, 35).

ACKNOWLEDGEMENTS

I wish to thank the members of the CELLO, JADE, MAC, MARK II, PLUTO, and TASSO collaborations and my colleagues from the MARK-II group for discussion and for providing me with unpublished data. In particular I am very grateful to H.-U. Martyn and B. Naroska for helpful comments and to D.P. Barber and R.R. Rau for critical reading of the manuscript. Finally, many thanks to the organizers of the 1982 SLAC Summer Institute on Particle Physics for their warm hospitality.

REFERENCES

- (1) For review see L.M. Sehgal, Aachen Report PITHA 80/17; P.-Q. Hung and J.J. Sakurai, Ann. Rev. Nucl. Sci. 31, 375 (1981); F.W. Büsser, Proc. of the Int. Conf. on Neutrino Physics and Astrophysics, Wailea, Hawaii, 1981; G. Barbieri, Proc. of the 1982 Int. Symp. on Lepton and Photon Interactions at High Energies, ed. W. Pfaill, Bonn 1981, p. 623; F. Niebergall, Proc. of Neutrino '82, Balatonfured 1982, to be published, and CERN preprint CERN-EP/82-105 (1981).
- (2) Y.F. Kim et al., Rev. Mod. Phys. 53, 211 (1981).
- (3) C.Y. Prescott et al., Phys. Lett. 77B, 347 (1978) and Phys. Lett. 84B, 524 (1979).
- (4) S.L. Glashow, Nucl. Phys. 22, 579 (1961); S. Weinberg, Phys. Rev. Lett. 19, 1264 (1967) and Phys. Rev. D5, 1412 (1972); A. Salam, in Elementary Particle Theory, ed. N. Svartholm, Stockholm 1968, p. 361; S.L. Glashow, J. Iliopoulos and L. Maiani, Phys. Rev. D2, 1285 (1970).

- (5) H. Faissner, New Phenomena in Lepton-Hadron Physics (1979), ed. D.E. Fries and J. Wess (Plenum Publishing Corp., New York), p. 371;
 H. Reichler, Phys. Blätter 25, 630 (1979);
 F.W. Bullock, Proc. of Neutrino 79, Bergen 1979, p. 398;
- (6) R.H. Feistelberg et al., Phys. Rev. Lett. 44, 635 (1980);
 M. Jonker et al., Phys. Lett. 105B, 242 (1981) and Phys. Lett. 117B, 272 (1982).
- (7) P. Q. Hung and J.J. Sakurai, Phys. Lett. 69B, 323 (1977).
- (8) CELLO Collaboration:
 H.J. Behrend et al., Phys. Lett. 103B, 148 (1981); Z. Phys. 14, 283 (1982), and DESY Report, DESY 82-027 (1982).
- (9) JADE Collaboration:
 W. Bartel et al., Phys. Lett. 88B, 171 (1979); Phys. Lett. 92B, 206 (1980); Phys. Lett. 99B 281 (1981); Phys. Lett. 108B, 140 (1982).
- (10) MARK-J Collaboration:
 D.P. Barber et al., Phys. Reports 63, 337 (1980); Phys. Rev. Lett. 42, 1110 (1979); Phys. Rev. Lett. 43, 1915 (1979); Phys. Lett. 95B, 149 (1980); Phys. Lett. 99B 495 (1981); Phys. Rev. Lett. 48, 1701 (1982).
- (11) PLUTO Collaboration:
 Ch. Berger et al., Z. Phys. C6, 269 (1980); Z. Phys. C1, 343 (1979); Z. Phys. C7, 289 (1981); Phys. Lett. 94B, 87 (1980); Phys. Lett. 99B, 489 (1981).
- (12) TASSO Collaboration:
 R. Brandelik et al., Phys. Lett. 83B, 261 (1979); Phys. Lett. 92B, 199 (1980); Phys. Lett. 94B, 259 (1980); Phys. Lett. 110B, 173 (1982); Phys. Lett. 117B, 365 (1982).
- (13) MAC Collaboration:
 J.G. Smith, Proc. of the XVII Rencontre de Moriond, ed. Tran Tan Van, Les Arcs 1982, p. 131;
 D.M. Ritson, Talk at the XXI Int. Conf. on High Energy Physics, July 1982, to be published in the Proceedings.
- (14) MARK II Collaboration:
 R. Rollebe, 1981 Int. Symp. on Lepton and Photon Interaction at High Energies, Bonn 1981, p. 1;
 J. Strait, Proc. of the XVII Rencontre de Moriond, ed. Tran Tan Van, Les Arcs 1982, p. 145.
- (15) F.A. Berends and R. Kleiss, Nucl. Phys. B177, 237 (1981).
 (16) R. Budny, Phys. Lett. 53B, 227 (1975)
- (17) F.A. Berends, R. Kleiss and S. Jadach, Leiden preprint.
- (18) T. Himel et al., Phys. Rev. Lett. 41, 449 (1978).
- (19) CELLO Collaboration:
 H.J. Behrend et al., Phys. Lett. 114B, 282 (1982).
- (20) MARK II Collaboration:
 C.A. Blocker et al., Phys. Lett. 49, 1369 (1982).
- (21) MARK-J Collaboration:
 J. Bürger, Talk at the XXI Int. Conf. on High Energy Physics, July 1982, to be published in the Proceedings.
- (22) C.A. Blocker et al., Phys. Lett. 109B, 119 (1982).
- (23) TASSO Collaboration: Phys. Lett. 92B, 199 (1980).
- (24) J.-J. Sakurai, Proc. of the XVII Rencontre de Moriond, ed. Y. Tran Tan Van, Les Arcs 1982, p. 241.
- (25) H. Georgi and S. Weinberg, Phys. Rev. D17, 275 (1978).
- (26) E.H. de Groot, G.J. Gounaris and D. Schildknecht, Phys. Lett. 85B, 399 (1979); Phys. Lett. 90B, 427 (1980) and Z. Phys. C5, 127 (1980);
 V. Barber, M. Keung, and E. Ma, Phys. Rev. Lett. 44, 1169 (1980);
 Phys. Lett. 94B, 377 (1980); Phys. Rev. D22, 727 (1980).
- (27) J. Ellis and M.K. Gaillard, CERN-Report CERN 76-18 (1976), p. 21.
- (28) JADE Collaboration:
 G. Heinzelmann, Talk at the XXI Int. Conf. on High Energy Physics, July 1982, to be published in the Proceedings.
- (29) TASSO Collaboration:
 R. Brandelik et al., Phys. Lett. 113B, 499 (1982).
- (30) J. Jersak, E. Laermann and P.M. Zerwas, Phys. Lett. 98B, 363 (1981).
- (31) A. Ali, Z. Physik, C1, 25 (1979);
 M.J. Puhalda et al., Phys. Rev. D25, 95 (1982) and Phys. Rev. D25, 695 (1982).
- (32) TASSO Collaboration:
 D. Hüke, Talk at the XXI Int. Conf. on High Energy Physics, July 1982, to be published in the Proceedings.

- (33) G.L. Kane and M.E. Peskin, Nucl. Phys. B195, 29 (1982).
- (34) B. Gittelman, Talk at the XXI Int. Conf. on High Energy Physics, July 1982, to be published in the Proceedings.
- (35) CELLO Collaboration:
H.J. Berend et al., DESY 82-021 (1982).
JADE Collaboration:
W. Bartel et al., Phys. Lett. 114B, 211 (1982).
MARK II Collaboration:
A. Blocker et al., SLAC-PUB-2923 (1982).
MARK-J Collaboration:
A. Adeva et al., Phys. Lett. 115B, 345 (1982).
TASSO Collaboration:
M. Althoff et al., DESY 82-69 (1982).